Seasonal variability of cyclone heat potential and cyclonic responses in the Bay of Bengal characterized using moored observatories

G. Vengatesan[1], P. Shanmugam[2], R. Venkatesan[1],
N. Vedachalam[*1] and Jossia K. Joseph[1]

[1]National Institute of Ocean Technology, Ministry of Earth Sciences, Chennai, India
[2]Indian Institute of Technology, Chennai, India

Abstract. Cyclone Heat Potential (CHP) is an essential parameter for accurate prediction of the intensity of tropical cyclones. The variability of the heat storage in the near-surface layers and the vertical stratification near the surface due to large fresh water inputs create challenges in predicting the intraseasonal and interannual evolution of monsoons and tropical cyclones in the Bay of Bengal. This paper for the first time presents the D26- referenced cyclone heat potential observed in the Bay of Bengal during the period 2012-17 based on the in-situ data collected from 5.5 million demanding offshore instrument-hours of operation in the Ocean Moored Buoy Network for Northern Indian Ocean (OMNI) buoy network by the National Institute of Ocean Technology. It is observed that the CHP in the Bay of Bengal varied from 0-220 kJ/cm² during various seasons. From the moored buoy observations, a CHP of ~ 90 kJ/cm² with the D26 isotherm of minimum 100m is favorable for the intensification of the post-monsoon tropical cyclones. The responses of the D26 thermal structure during major tropical cyclone events in the Bay of Bengal are also presented.

Keywords: Bay of Bengal; Cyclone Heat Potential; Tropical cyclones; OMNI Buoy

1. Introduction

A timely and precise weather forecast is the key requirement for a successful ocean observation program. Precise spatio-temporal measurements of meteorological and oceanographic parameters are essential for the effective cyclone tracking and intensity predictions.The Bay of Bengal (BoB), the north-eastern limb of the tropical Indian Ocean, is a region which is strongly coupled with summer and winter monsoons and intense tropical cyclones (TC) as described in Venkatesan (2016).The Bay is also a region of strong vertical stratification near the surface due to large inputs of freshwater through rainfall and river run-off. As a result, BoB is normally prone to TC during the pre-monsoon months of April–May and the post-monsoon months of October–November as indicated in Weller (2016). During the post-monsoon period, the BoB is pre-conditioned by warm sea surface temperature (SST) > 30ºC which is highly conducive for the TC formation as described

---

in Chaitanya *et al*. (2015). Over the past two decades, in order to collect increased spatiotemporal meteorological, water surface and sea sub-surface parameters in near-real time, the moored buoys have been deployed by National Institute of Ocean Technology (NIOT) in more than 650 locations ranging from the coastal waters to the deep oceans spanning between 63–93°E and 6–20°N. The collected data are transmitted by INMARSAT to the mission control center (MCC) at NIOT in Chennai and to the Indian Tsunami Early Warning Center (ITEWC) in Indian National Center for Oceanic Information Systems (INCOIS), Hyderabad as described in Venkatesan (2018, 2013) and Kumar *et al*. (2016).

The Ocean Moored Buoy Network for Northern Indian Ocean (OMNI) is developed and operated by NIOT since 2010 for mainly understanding the variability in the upper ocean thermohaline and current structure on varied time scales, which has important bearing on the evolution of seasonal monsoons and TC in the BoB and Arabian Sea as detailed in Venkatesan (2013). This paper presents the D26-referenced cyclone heat potential (CHP) observed in the northern, central and southern BoB using the OMNI buoy network during the period 2012-17 and the oceanic subsurface responses of the D26 thermal structure during major TC events.

2. Description of moored observation system

The architecture of the OMNI buoy is shown in Fig.1. A system comprising of a poly-urethane foam-filled fiber reinforced plastic hull is moored to the seabed using a dead weight and an anchor in an inverse catenary configuration. The mooring comprises of a negative buoyant wire rope, a nylon rope, and positive buoyant polypropylene (PP) rope, suitable connectors like shackles and swivels as detailed in Venkatesan (2013b).
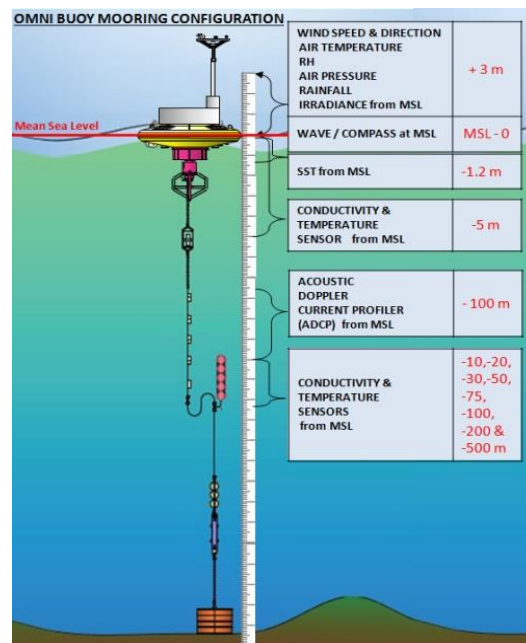

Fig. 1 Configuration of the OMNI moored buoy, Venkatesan (2013,2016, 2017)

Fig. 2 OMNI buoy being deployed from ORV Sagar Kanya, Venkatesan (2013,2016, 2017)

The chain attached to the dead weight and the PP rope is held in an upright position using a group of subsurface floats. A combination wire rope which has PP sheathing on the metal rope is used for interconnecting the surface buoy and the nylon rope as detailed in Venkatesan (2015). The central cylinder in the buoy houses batteries, data acquisition system (DAS) and associated electronics. The buoy power system comprises of solar-powered lead-acid batteries backed with lithium-thionyl chloride (LiSoCl2) batteries as in Venkatesan (2015). The meteorological and sea surface instruments are connected to the DAS. The surface and subsurface instruments that are positioned at 5, 10, 20, 30, 50, 75, 100, 200 and 500 m water depths are interfaced with the DAS using induction mooring which helps to reduce the underwater connectors and hence increase the reliability. An electronic controller unit with 3-level software-based watchdog timer, rebooting facility and the two-way communication feature between the buoy and the MCC enabling forced restart facility helps to achieve the highest level of system on-demand reliability and availability. The position moorings that are designed using advanced numerical modeling aids, deployed scientifically and monitored from the MCC, have achieved a mean time between the failures (MTBF) of about 12 years. The unattended OMNI buoy reporting every 3 hours to the MCC ensures the system compliance with the most stringent IEC 61508 Safety Integrity Level 4 and the reliability aspects are detailed in Venkatesan *et al*. (2016b). The deployed view of the OMNI buoy is shown in Fig. 2.

The instruments used in the OMNI buoys are selected based on the proven reliability and sensor stability in similar systems such as the RAMA/TAO/TRITON/ATLAS/PIRATA data buoys (Hermes *et al*. 2019, Karmakar *et al*. 2018, Cyriac *et al*. 2019). The instrumentation calibration procedures and accuracy estimate of the meteorological and oceanographic sensors are set to follow the best of practices published by the National Oceanic and Atmospheric Administration (NOAA)/Pacific Marine Environmental Laboratory (PMEL) Ando *et al*. (2017), Bourlès *et al*. (2008), McPhaden *et al*. (1998). The sensor selection and application practices have matured based on the return of experiences from more than 457 field underperformances observed in the meteorological, sea surface and sea subsurface instruments that have clocked about 7.3 million demanding offshore instrument-hours during the period 1997-2018 as described in (Venkatesan *et al.* 2017a, b).

The achieved MTBF of the buoy integrated cyclone monitoring sensor suite of 0.6 years and the identified offshore failure modes forms the basis of the reliability-centered instrument integrity management program. The implemented integrity management program includes continuous sensor operation monitoring, annual 4-slot offshore field maintenance program, sensor data quality assurance feature using Advanced Data Reception and

Analysis System (ADDRESS), redundant sensor configuration and the remote video surveillance system as detailed in Venkatesan (2015, 2017). Various techno-management strategies are continuously adopted for increasing the data returns and optimizing the offshore system maintenance costs.

Since its inception, the buoy network has recorded 22 cyclonic events including the very severe cyclones Phailin in 2013, Hud-Hud in 2014 and the Vardha in 2016. Seven buoys enabled efficient and precise tracking of the Phailin cyclone from evolution till land fall, and the sensors provided valuable information for future cyclone prediction modeling which is described in Venkatesan *et al.* (2014). The data acquired during various events served as important inputs to various agencies including the Indian Meteorological Department (IMD) and for understanding the Indian Ocean dynamics which is essential for improved modeling of the evolution of the seasonal monsoons and cyclones as described in Mathew *et al.* (2018) and Kumar *et al.* (2017). The super-computer Pratyush established at the Indian Institute of Tropical Meteorology (IITM) in Pune and the National Center for Medium Range Weather Forecasting (NCMRWF) in Noida augments India's capability in improving the weather and climate forecasting services and described in Vedachalam (2018).

3. CHP and its importance in the BoB

The favorable conditions for the formation of TC are low level vorticity, coriolis parameter, inverse of the vertical shear of the horizontal wind between the lower and upper troposphere, sea temperature in excess of 26°C to a depth of 60 m indicated as D26 isotherm, vertical gradient of the temperature between the surface and 500 mb, and mid-troposphere relative humidity. The intensification of TC is caused by the interaction of complex mechanisms including TC dynamics, upper-ocean interaction and the atmospheric circulation. Although in the past two decades there is a steady improvement in the cyclone track prediction, improvement on the cyclone intensity prediction is still highly challenging.

Studies on understanding the intensification of TC based on the concept of Cyclone Heat Potential (CHP) and the D26 isotherm was first propounded by Palmen in 1948. He postulated that TC forms over regions where SST is > 26°C, which was subsequently accepted as a threshold for the genesis of TC as described in Palmen (1948). The cooling of the upper ocean due to TC-induced mixing and impacting the cyclone intensity is based on the principle of the Carnot heat engine in which energy added at the underlying warm ocean surface is transferred to the developing cyclone as described in Robert (2008). In 1972, the D26 isotherm was classically used by Leipper and Volgenau (1972) to calculate the CHP for the hurricanes generated in the Gulf of Mexico. Studies by Sadhuram and Murthy (2006), revealed good association between the CHP and the efficiency of the TC intensification. Sadhuram *et al.* (2010) and Manesha *et al.* (2015) analyzed 15 cyclones during 1990-2006 for understanding the importance of upper ocean heat content in the intensification and translation speed of the cyclones over the BoB. Ho *et al.* (2011) analyzed 35 typhoons in the western Pacific during 2006-2009 and reported a correlation coefficient of more than 0.8 between the TC intensity and the accumulated CHP.

Krishna *et al.* (2012) analyzed the response of the upper ocean during the passage of the MALA cyclone using ARGO data and identified that the CHP and the depth-averaged temperature has a good correlation.

Lin *et al.* (2013), analysed the storm surge events associated with severe hurricanes Katrina and Nargis, and identified that higher CHP favors intensification. Maneesha (2012, 2015) described the role of upper ocean parameters in the genesis, intensification and tracks of the TC over the BoB. Sankar Nath (2016) examined the inter-decadal variations of the TC activity and CHP over the BoB for the post-monsoon season during the period 1955-2013. Krishnamurti *et al.* (2017) analyzed the monsoonal interseaosnal oscillations in the ocean heat content over the surface layers of the BoB based on 17 years data and identified a strong correlation to the intersessional oscillations of rainfall.

Anastassia et al. (2017) indicated that the water vapor budget of a hurricane is dependent on its movement and the importance of the atmospheric moisture stocks and dynamics in the behavior of TC. Studies by Wang (2008) indicated that air-sea interactions with high values of CHP were the reason behind the rapid intensification of the typhoon Fenshen. Thus, the thermal energy needed for the development of TC, monsoons, as well as any prolonged marine weather event comes from the layers in the upper ocean and not from the thin layer represented by SST. Hense, the intensification of most TC is linked to the variability of the integrated vertical temperature under the storm track.

Because of the unique geography of the Northern Indian Ocean, during spring (April-May) and fall (Oct-Dec) seasons, the region between 10° and 15°N gives rise to several depressions of which few intensify into severe and very severe storms. Thus, monitoring the seasonal variability of the CHP in the BoB is essential for precisely predicting the intensification of the TC.

The CHP, as defined in equation 1 and represented in Fig. 3, is the integral temperature in excess of 26°C up to a depth of 26° isotherm as described in Palmen (1948).

$$CHP = \rho Cp \int_0^{D26} (T - 26) dz \qquad (1)$$

where ρ is the density of sea water in kg/m^3, Cp is the specific heat capacity of sea water, T is the temperature corresponding to the layer at depth z, D26 is the depth of the 26ºC isotherm.

During a passing TC, wind is the important factor contributing the sea-air energy exchange. The wind stress is calculated based on the wind velocity as described in Reddy (2018)

$$\tau = CD\rho U^2 \qquad (2)$$

Where in Eq. (2), U is the wind speed measured at 10 m from the sea surface, density of air 1.22 kg/m³ and Cd is the drag coefficient of 0.0013.
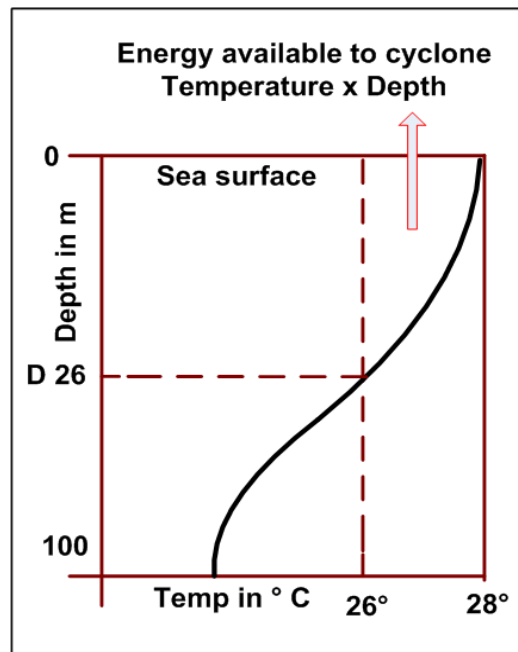

Fig. 3 Representation of the D26 isotherm

4. Study locations and observations

The locations in which the OMNI buoys are deployed in the Indian Ocean marginal seas for monitoring the meteorological and oceanographic parameters during the period 2012-2018 are shown in Fig. 4. The details of the WMO ID, location and depth of deployment of the OMNI buoys are given in Table 1.
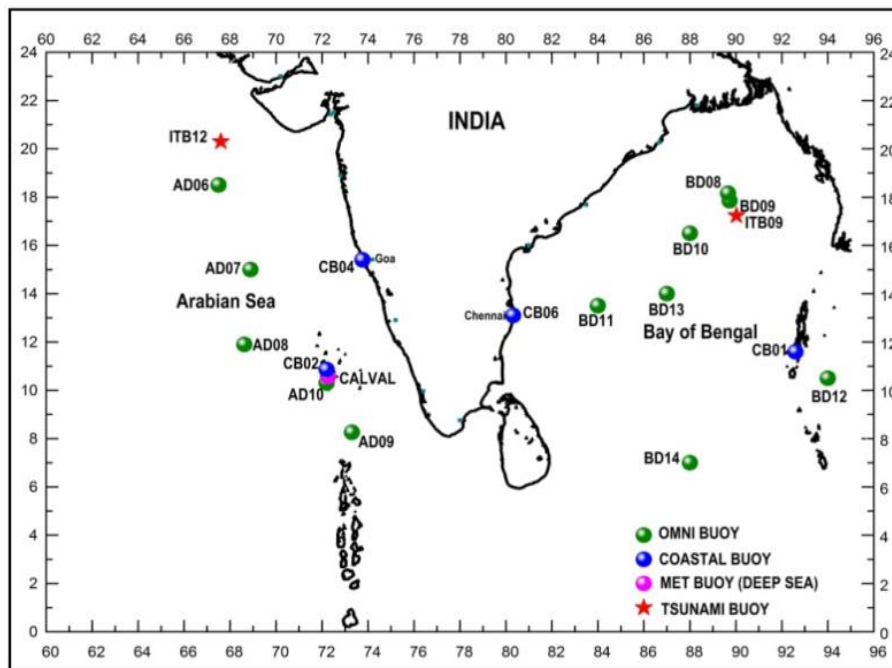

Fig. 4 Study locations in the BoB

Table 1 Details of the OMNI buoys in the study locations

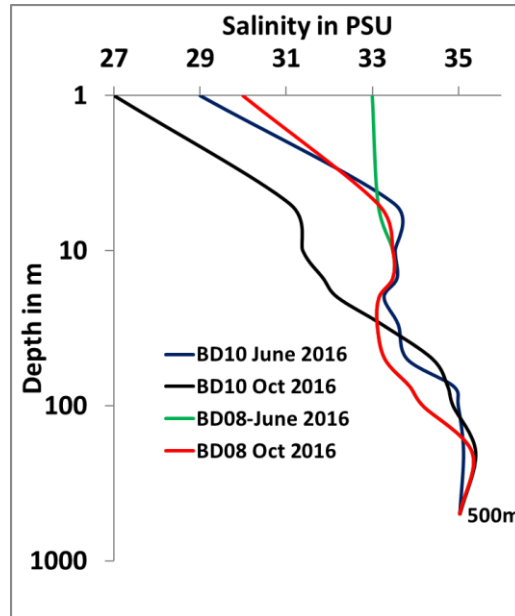| NIOT Buoy ID	WMO ID	Latitude (N)	Longitude (E	Depth m
BD08	23091	18°10'16"	89°40'12"	2110
BD10	23093	16° 21' 16	87° 58' 21"	2640
BD11	23094	14°12'10"	82°54'11"	3369
BD12	23095	10° 30' 13"	94° 02' 6"	3050
BD13	23459	14° 02' 01"	87° 00' 02"	3000
BD14	23460	08°10'35"	85°29'53"	3740

Fig. 5 Salinity variation (averaged) in the BoB

5. Observations and discussion

The salinity measurements made by the buoys in the northern BoB during 2012-17 (averaged) is plotted in Fig. 5. The heavy rainfall and enhanced discharge of major rivers such as Ganges-Brahmaputra and the Irrawaddy till October lead to dramatic surface freshening within the BoB resulting in a strong salinity stratification in the surface. The salinity stratification can therefore have a two-fold impact on SST. The shallow layer traps the atmospheric heat flux, leading to enhanced SST variability. This barrier layer suppresses heat exchange between the warm mixed layer and the cold thermocline, which is essential for maintaining the high SST and convective activity during the monsoon and has the TCHP, which is the capability of the near sea surface to supply rapid energy to the developing tropical cyclones.

5.1 Northern BoB- 18°10'16"- 89°40'12" (BD08)

The observations by buoy the located in the North Bay location are plotted in Fig. 6. During winter (Jan-Feb), the location is characterized by lower CHP ranging 0-40 kJ/cm². The CHP recorded in 2013 was the lowest during the period 2012-16. During the pre-monsoon period, the CHP increases gradually and ranges between 50 and 100 kJ/cm². In 2014, the highest CHP of 180 kJ/cm²was observed. During the south-west (SW) monsoon season, the CHP varied from 40-60 kJ/cm².

5.2 Northern BoB - 16° 21' 16- 87° 58' 21"(BD10)

The observations by the buoy BD10 (located south of the buoy identified as BD08) are shown in Fig. 7. During winter, the location is characterized by CHP ranging from 0 to 60 kJ/cm². During the pre-monsoon period,

the CHP increased gradually in the range 50-100 kJ/cm². The highest CHP of 220 kJ/cm² is observed. During the SW monsoon season, the CHP varied between 50 and 75 kJ/cm². The average CHP observed during the period 2012-16 was about 50 kJ/cm².

5.3 Central BoB- 14°12'10"- 82°54'11" (BD11)

The observations by buoy BD11 in the Central Bay are shown in Fig. 8. During winter, the central bay is characterized by the CHP ranging 0-50 kJ/cm². During 2014 and 2015, the CHP was around 20 kJ/cm². During the pre-monsoon period, year 2016 recorded a highest CHP of 190 kJ/cm², while the other years recorded the CHP between 50 and 110 kJ/cm². During the SW monsoon period, the CHP gradually decreased and varied between 40 and 60 kJ/cm².

5.4 Central BoB - 14° 02' 01"- 87° 00' 02" (BD13)

The observations by BD13 in the Central bay are shown in Fig. 9. During winter, the central bay was characterized by CHP ranging between 10 and 60 kJ/cm². During 2012 and 2016, the CHP was slightly higher than the observations in other years. During the pre-monsoon period, the year 2016 recorded a highest CHP of ~200 kJ/cm². During the SW monsoon season, the CHP was the highest in 2016, which was ~ 100 kJ/cm².
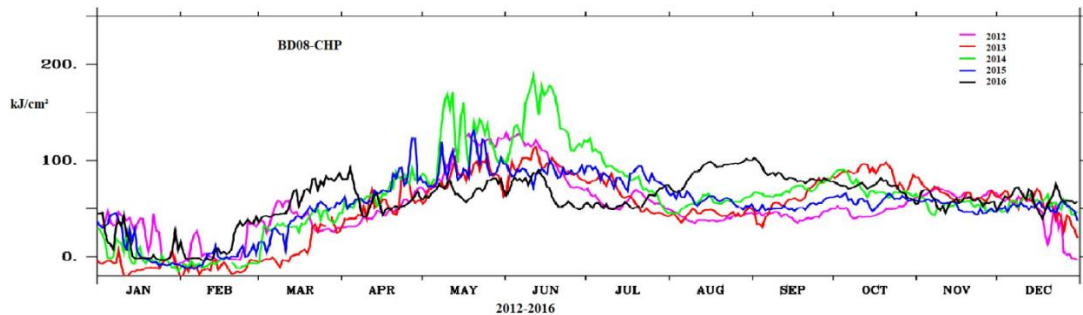

Fig. 6 CHP observations in the northern location BoB (BD08) during 2012-2016
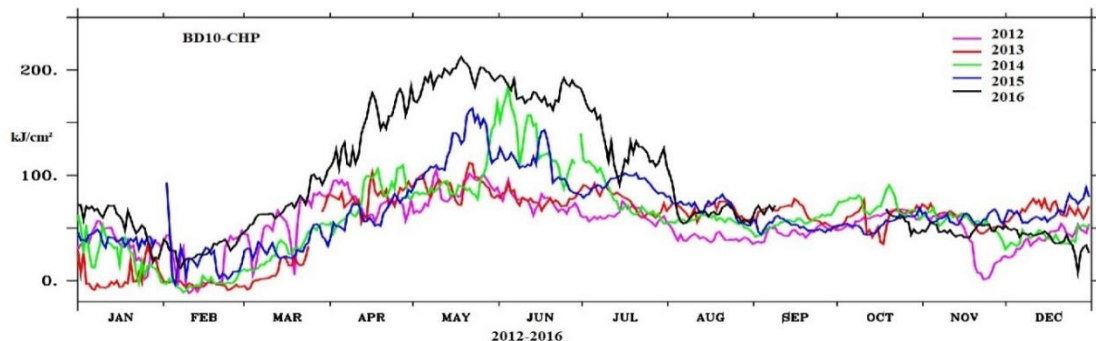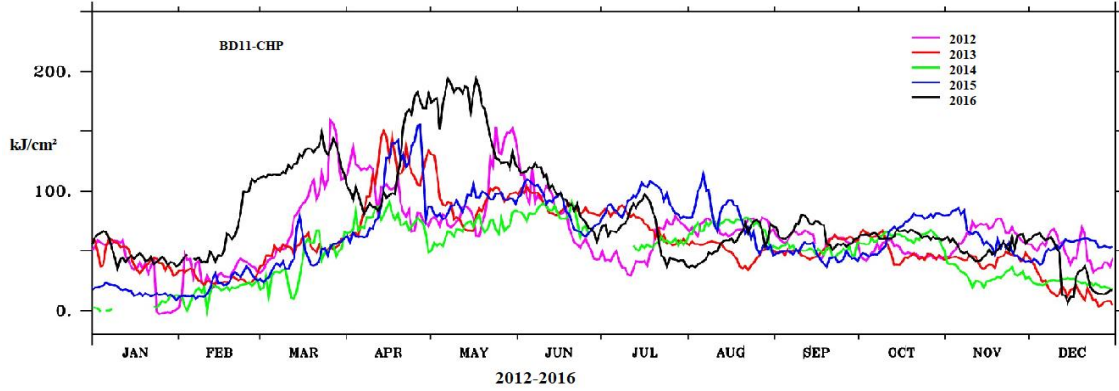

Fig. 7 CHP observations by BD10 during 2012-2016

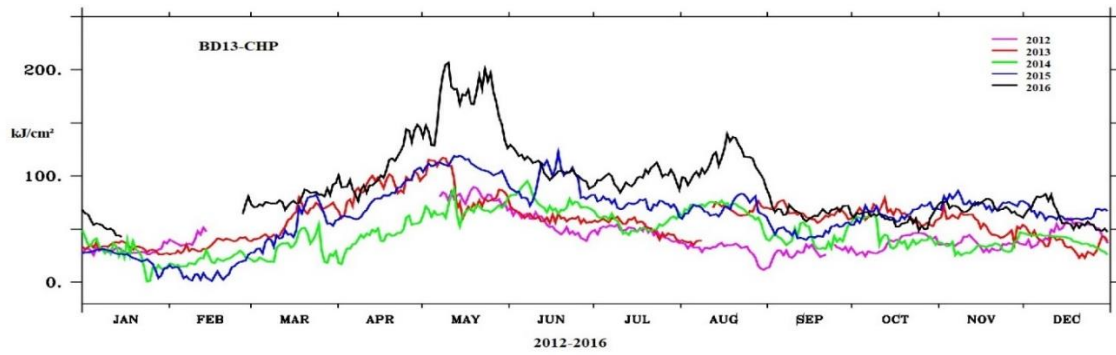Fig. 8 CHP observations by BD11 during 2012-2016
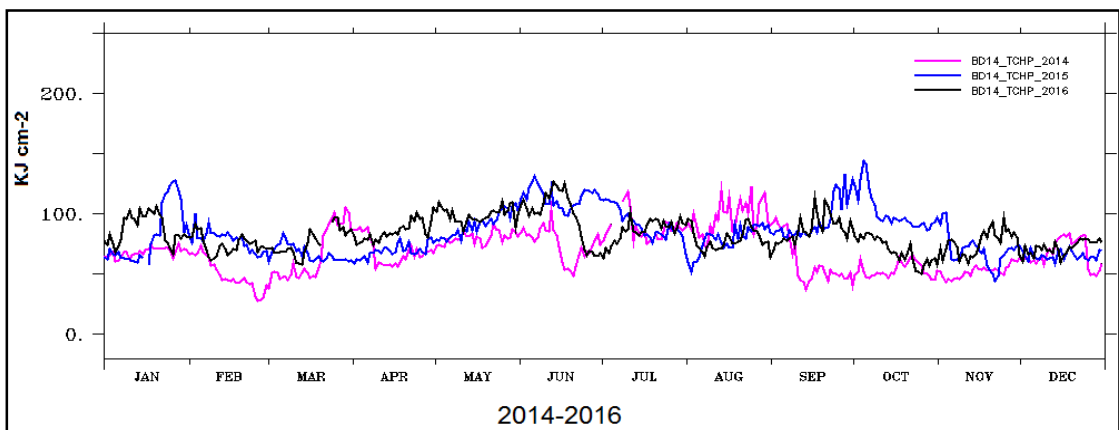

Fig. 9 CHP observations by BD13 during 2012-2016

Fig. 10 CHP observations by BD14 during 2014-2016

5.5 Southern BoB- 08°10'35"- 85°29'53" (BD14)

The observations from the buoy BD14 located in southern bay are plotted in Fig. 10. It was observed that the southern bay was characterized by the CHP in the range 40-100 kJ/cm²throughout the year. The same trend was observed in all the four years. Some of the post monsoon TC originated from this region.

5.6 CHP variation Near Andaman Sea- 10° 30' 13" -94° 02' 6" (BD12)

The observations from the buoy BD12 in the location near the Andaman Sea are shown in Fig. 11 In this region, the CHP remained fairly between 50 and 100 kJ/cm² during all the four years. During the pre-monsoon period, the CHP was observed around ~ 80 kJ/cm². During the month of August, CHP varied between 50 and 100 kJ/cm² and most of the post-monsoon cyclone genesis were centered on this location. During the SW monsoon season, the highest TCHP was ~ 80 kJ/cm².

The variability in the CHP and depth of the D26 isotherm during various seasons during the period 2012-17 is shown in Fig. 12.

The summary of the spatio-temporal CHP observations made in the northern, central, southern and near the Andaman sea during various seasons are represented in Table 2. The depth of the D26 isotherm average value is indicated within brackets.

6. Observed CHP response during TC

The trajectories of the pre-monsoon and the post monsoon TC in the BoB during the period 2012-2016 are shown in Figs. 13 and 14, respectively. The buoy traces of the TC and the observations made by the Indian Meteorological Department (IMD) during these periods are summarized in Table 3. From the list of very sever cyclones (Table.4), the observations of SST, wind and the CHP during the passage of two post monsoon very severe cyclonic storms (VSCS) – Vardha and Phailin and one pre-monsoon cyclone Viyaru are also presented as case studies.
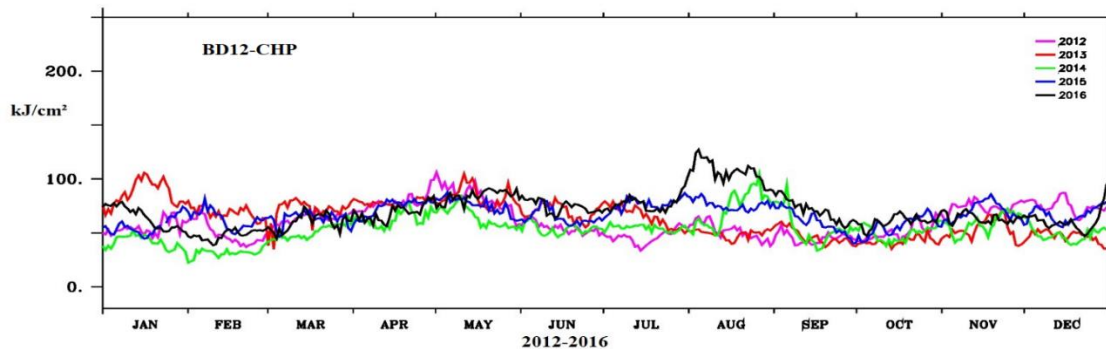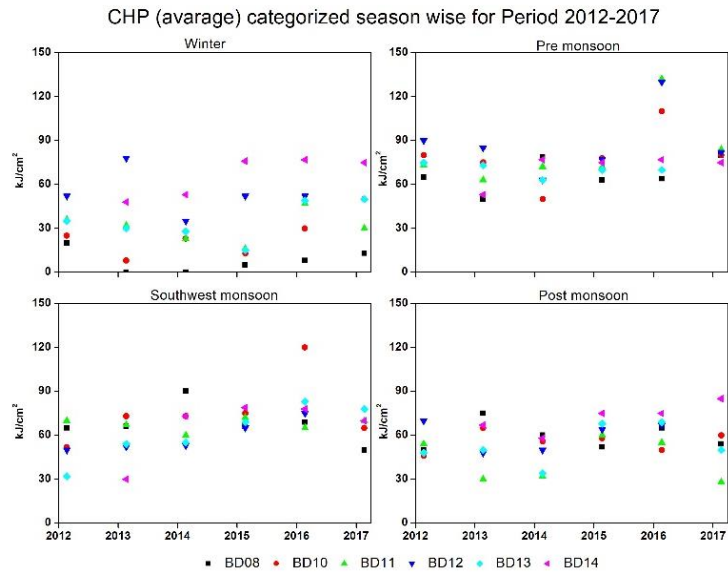

Fig. 11 CHP observations by BD12 during 2012-2016

Table 2 Characterized spatio-temporal variability of CHP in the BoB

Cyclone Heat Potential in kJ/cm²		
Winter	**Pre-monsoon**	**Post-monsoon**
North Bay 18°10'16"- 89°40'12"		
0-40 (10-50 m)	50- 100, 180 in 2014 (55-80 m)	40-60 (55- 80 m)
North Bay 16° 21' 16- 87° 58' 21"		
0-60 (10-50 m)	50- 100, 220 in 2016 (55-110 m)	50-75 (40-60 m)
Central Bay 14°12'10"- 82°54'11"		
0-50 (25-55 m)	50- 70. 190 in 2016 (60-90 m)	40-60 (30-65 m)
Central Bay 10° 30' 13" - 94° 02' 6"		
10-60 (25-55 m)	50- 70, 200 in 2016 (70-120 m)	40-100 (35-70 m)
South Bay 14° 02' 01" - 87° 00' 02"		
60-100 (50-90 m)		
Near Andaman sea 08°10'35"- 85°29'53"		
65-105 (50-100 m)		

CHP (avarage) categorized season wise for Period 2012-2017
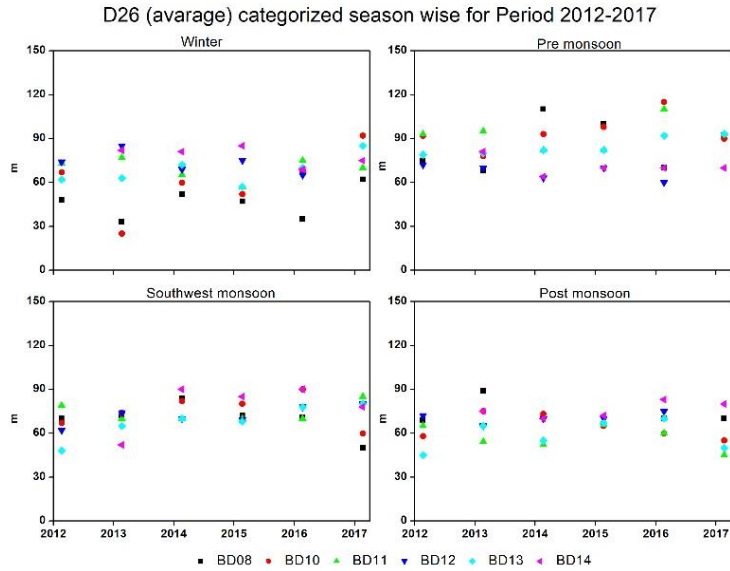
Continued-

Fig.12 CHP and depth of the D26 isotherm during various seasons during the period 2012-17
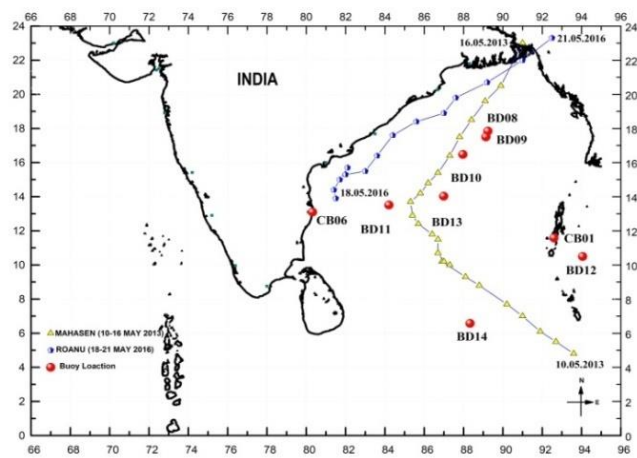

Fig. 13 Pre-monsoon TC trajectory during 2012-2016

Case study 1: Extreme severe cyclonic storm Phailin

The Phailin is the extremely severe cyclonic storm in the BoB during post monsoon season in 2013 with wind speeds reaching 215km/hr during landfall. The BD10 buoy which was within the eye of the cyclone recorded a minimum atmospheric pressure of 920hPa. It is the lowest value recorded till date by any instrument in the northern Indian Ocean. When the cyclone crossed BD10, the SST was around 29ºC, TCHP was 120 kJ/cm² and the depth of the D26 isotherm was 120m. During the same day, the NOAA database indicated a TCHP of

~110 kJ/cm² in the northern bay. During the passage of the cyclone with a wind stress of 2 N/m², the surface temperature dropped by 0.7°C and isotherm depth increased to 60m. After the passage of the cyclone, the CHP reduced to ~40 kJ/cm² resulting in a reduction by ~80 kJ/cm². The high CHP along with highly stratified waters in the northwestern BoB favored the intensification of cyclone as described in Venkatesan (2014). The observations are represented in Fig.15.

Table 3 Major Cyclones traced by the buoys during 2012-16

Name of cyclone	Period	Buoy trace	IMD Observation
Nilam Cyclonic Storm	Oct 10,2012	BD13, BD11	85km/h, 987 hpa
Viyaru Cyclonic Storm	May 10-17 2013	BD08, BD09, BD10, BD11, BD13, BD14	85km/h, 990 hpa
Phailin Very Severe Cyclonic Storm	Oct 8-14 2013	CB01, BD08, BD09, BD10, BD13	215km/h, 920 hpa
Helen Severe Cyclonic Storm	Nov 19- 23 2013	BD11, CB05	100km/h, 990 hpa
Lehar Very Severe CycloStorm '	Nov 23-29 2013	CB01, BD11, BD12, BD13	140km/h, 980 hpa
Madi Very Severe Cyclonic Storm '	Dec 6-15 2013	CB05, BD11	120km/h, 986 hpa
Hudhud Very Severe Cyclonic Storm	Oct 6-14 2014	CB01, BD08, BD09, BD10, BD11, BD12, BD13	85km/h , 950 hpa
Roanu Cyclonic Storm	May 17-22, 2016	CB06, BD11, BD10, BD09, BD08	85km/h, 983 hpa
Kyant Cyclonic Storm	Oct 21-28, 2016	BD09, BD10, BD11, BD08	85km/h, 983 hpa
Nada Cyclonic Storm	Nov 29-Dec 2, 2016	CB06, BD14	75km/h,1000 hpa
Vardah Very Severe Cyclonic Storm	December 6 - 13, 2016	CB01, BD11, BD13, CB06	132km/h, 980 hpa

Table 4 Buoy observations on very severe cyclones during 2012-16

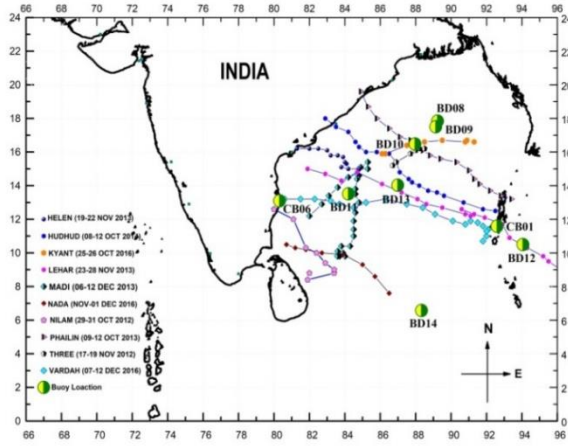| TC	Buoy WMO ID	Location		Distance from eye of cyclone (nm)	Wind stress in N/sq.m measured by buoy
		Lat	Lon		
Phailin	23093	16° 21' 16	87° 58' 21"	4	2
Vardhah	23094	14°12'10"	82°54'11"	31	1.2
Viraiyu	23459	14° 02'01"	87° 00' 02"	20	1.1
Lehar	23459	14° 02'01"	87° 00' 02"	19	1.1
HudHud	23459	14° 02'01"	87° 00' 02"	43	0.2

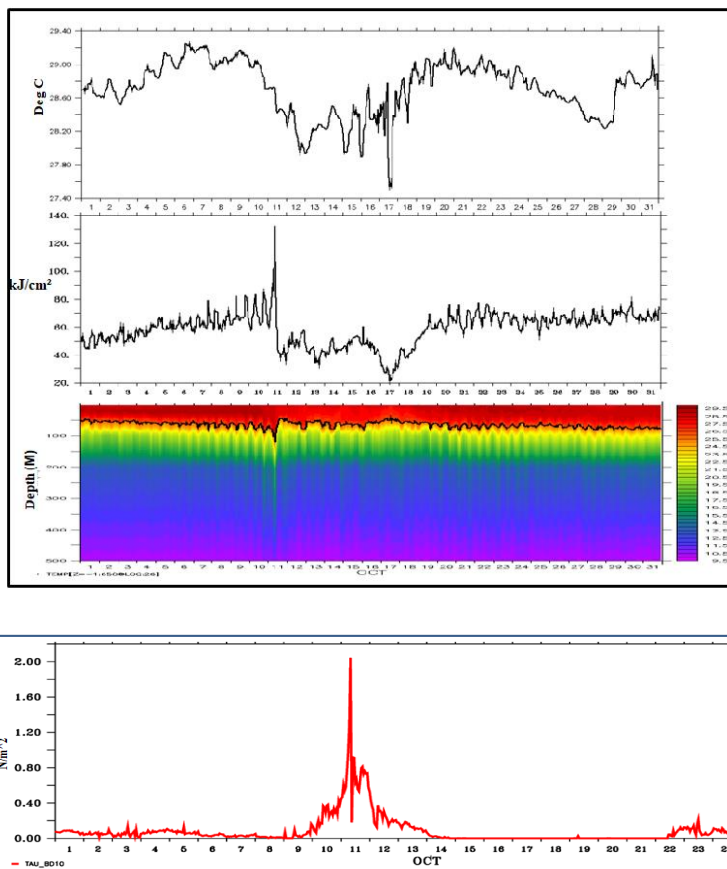Fig. 14 Post monsoon TC trajectory during 2012-2016

Fig. 15 SST, CHP, D26 and wind stress observations during Phailin cyclone by BD10
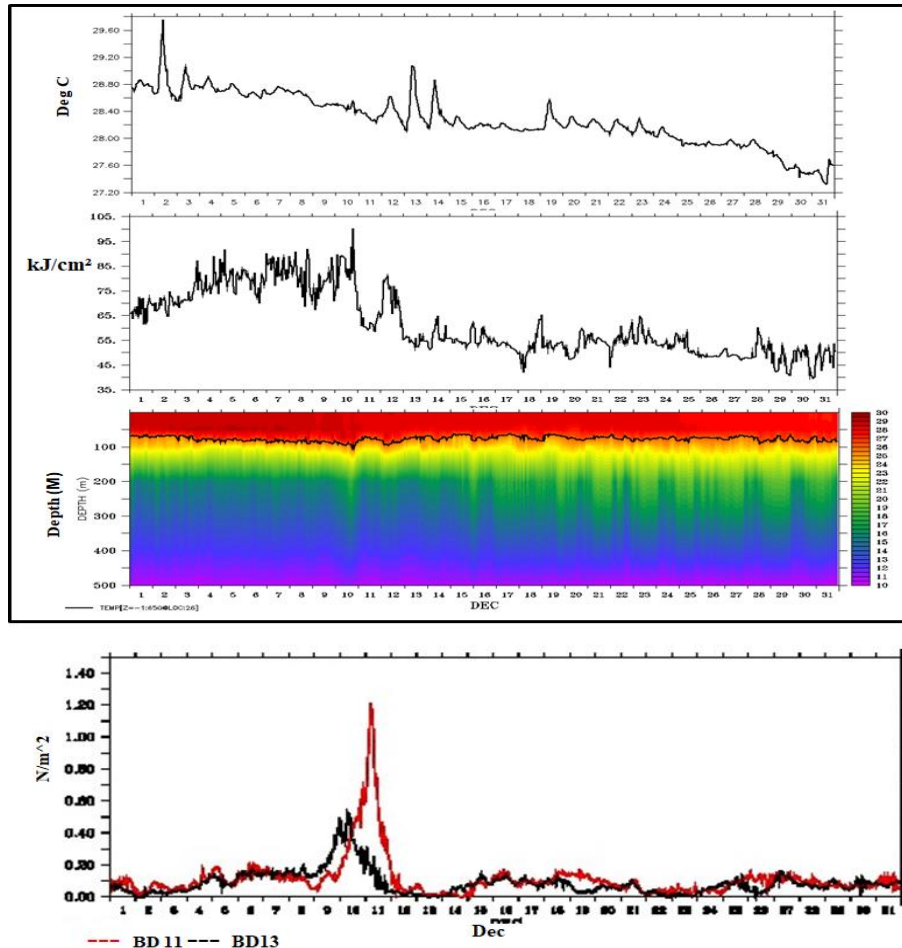
Fig. 16 SST, CHP, D26 and wind stress observations during Vardah cyclone by BD13

Case study 2: Very severe cyclonic storm (VSCS) Vardah

The Vardah which had its genesis in the south Andaman sea is the third post-monsoon season VSCS during 2016. The observations of BD13 during the passage of the VSCS are represented in Fig.16 using NOAA-PMEL software Ferret. Prior to the passage of VSCS Vardah on Dec 11, BD13 recorded a SST of 28°C, CHP was ~85 kJ/cm² and the D26 isotherm was at a depth of 60m. During the same day, the NOAA database indicated an SST of 28.5°C, CHP was ~80 kJ/cm² in the central bay.

During the passage of the VSCS Vardah, BD13 recorded a rapidly increasing wind stress of 1.2 N/m². The drop-in surface temperature by more than 2°C was due to the increased wind driven mixing. The CHP was more than 95kJ/cm² and the isotherm depth increased to 100m which shows the severe intensity of the cyclone. After the passage of the cyclone, the CHP reduced to ~50 kJ/cm² resulting in a CHP reduction by ~35kJ/cm².
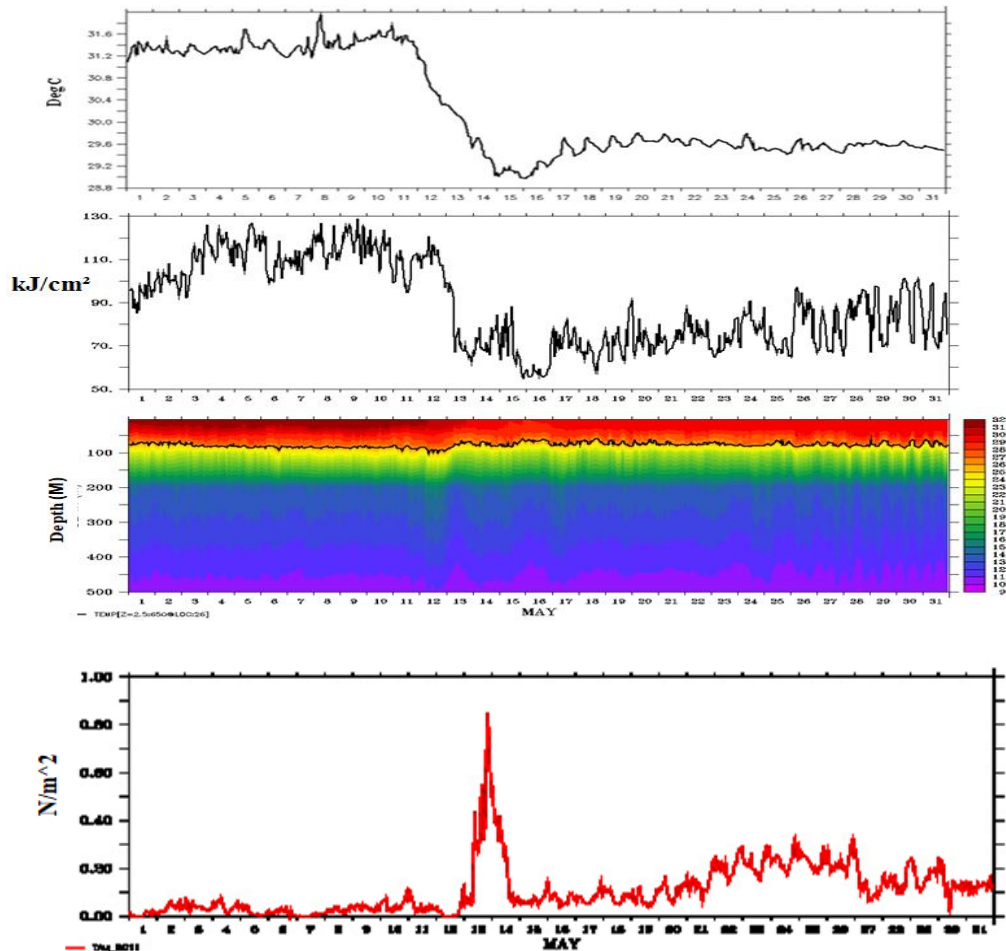
Fig. 17 SST, CHP, D26 and wind stress observations during Viyaru cyclone by BD13

Case study 3: VIYARU Cyclone

The Cyclone VIYARU was the first pre-monsoon TC in the BoB in 2013 which originated from a low pressure area that formed at 5°N and 92°E. It gradually drifted northwest and intensified into a cyclonic storm on 10 May 2013. The BD13 buoy which was on the track of the cyclone recorded minimum atmospheric pressure of 993 hPa. When the cyclone crossed BD13, the SST was around 31°C and the CHP was 120 kJ/cm². The depth of the isotherm was 100m and the wind stress was 0.8 N/m². During the same day, the NOAA database indicated a SST of 28.5°C, CHP was ~110 kJ/cm² in the central bay. After the passage of the VIYARU cyclone, the CHP reduced to ~70 kJ/cm². Due to the low winds no significant change in the depth of the D26 isotherm was observed. The observations are represented in Fig. 17.

7. Conclusions

Improvement in the tropical cyclone intensity forecasts is currently a top priority among the research community. The recent advances in the observational technologies in the fields of sensors, offshore platforms and real-time communication now provide unprecedented capability to monitor changes in our oceans and atmosphere that present new opportunities to understand the role of the oceans on climate change. From the in-situ CHP data acquired by the OMNI buoy network, it is observed that the CHP in the Bay of Bengal varied from 0-220 kJ/cm² during various seasons.   From the moored buoy observations, it is identified that a CHP of ~ 90 kJ/cm² favours of intensification of post-monsoon cyclones. The observations in the buoy located in the north bay at 16° 21' 16 N, 87° 58' 21" E location recorded a CHP of 220 kJ/cm² in 2016 and this indicates that 2016 is the warmest year during the period 2011-2016. The in-situ CHP data acquired by the OMNI buoy network in the Bay of Bengal and presented in this paper helps oceanographers in understanding the ocean-atmosphere interactions during the tropical cyclone intensification more precise. Considering the importance of CHP, NIOT is planning for providing CHP data to the stakeholders for enabling precise estimation of the tropical cyclone intensities and weather patterns.

Acknowledgements

References

Ando, K., Kuroda, Y., Fujii, Y., Fukuda, T., Hasegawa, T., Horii, T., Ishihara, Y., Kashino, Y., Masumoto, Y., Mizuno, K. and Nagura, M. (2017), "Fifteen years progress of the TRITON array in the Western Pacific and Eastern Indian Oceans", *J. Oceanography*, **73**(4), 403-426.

Bourlès, B., Lumpkin, R., McPhaden, M.J., Hernandez, F., Nobre, P., Campos, E., Yu, L., Planton, S., Busalacchi, A., Moura, A.D. and Servain, J. (2008), "The PIRATA program: History, accomplishments, and future directions", *Bull. Am. Meteorol. Soc.*, **89**(8), 1111-1126.

Chaitanya, A.V.S., Durand, F., Mathew, S., Gopalakrishna, V.V., Papa, F., Lengaigne, M., Vialard, J., Kranthikumar, C. and Venkatesan, R. (2015), "Observed year-to-year sea surface salinity variability in the Bay of Bengal during the 2009-2014 period", *Ocean Dynam.*, **65**(2), 173-186.

Cyriac, A., McPhaden, M.J., Phillips, H.E., Bindoff, N.L. and Feng, M., "Seasonal evolution of the surface layer heat balance in the eastern subtropical Indian Ocean", *J. Geophys. Res: Oceans*.

Ho, C.R., Tsao, Y.H., Kuo, N.J. and Huang, S.J. (2011), "Estimation of Tropical Cyclone Heat Potential from Oceanic Measurements", *Proceedings of the ASME 2011 30th International Conference on Ocean, Offshore and Arctic Engineering (pp. 817-822). American Society of Mechanical Engineers Digital Collection*.

Hermes, J.C., Masumoto, Y., Beal, L., Roxy, M., Vialard, J., Andres, M., Annamalai, H., Behera, S., d'Adamo, N., Feng, M. and Han, W. (2019), "A sustained ocean observing system in the Indian Ocean for climate related scientific knowledge and societal needs", *Front. Marine Sci.*, **6**, 355.

Jangir, B., Swain, D. and Bhaskar, T.U. (2016), May. Relation between tropical cyclone heat potential and cyclone intensity in the North Indian Ocean. In Remote Sensing and Modeling of the Atmosphere, Oceans, and Interactions VI (Vol. 9882, p. 988228). International Society for Optics and Photonics.

Krishnamurti, T.N., Jana, S., Krishnamurti, R., Kumar, V., Deepa, R., Papa, F., Bourassa, M.A. and Ali, M.M.

(2017), "Monsoonal intraseasonal oscillations in the ocean heat content over the surface layers of the Bay of Bengal", *J. Marine Syst.*, **167**, 19-32.

Kumar, M.R., Pinker, R.T., Mathew, S., Venkatesan, R. and Chen, W. (2018), "Evaluation of radiative fluxes over the north Indian Ocean", *Theor. Appl. Climatology*, **132**(3-4), 983-988.

Karmakar, A., Parekh, A., Chowdary, J.S. and Gnanaseelan, C. (2018), "Inter comparison of Tropical Indian Ocean features in different ocean reanalysis products", *Climate Dynam.*, **51**(1-2), 119-141.

Leipper, D.F. and Volgenau, D. (1972), "Hurricane heat potential of the Gulf of Mexico", *J. Phys. Oceanography*, **2**(3), 218-224.

Lin, I.I., Goni, G.J., Knaff, J.A., Forbes, C. and Ali, M.M. (2013), "Ocean heat content for tropical cyclone intensity forecasting and its impact on storm surge", *Natural Hazards*, **66**(3), 1481-1500.

Makarieva, A.M., Gorshkov, V.G., Nefiodov, A.V., Chikunov, A.V., Sheil, D., Nobre, A.D. and Li, B.L., (2016), "The water budget of a hurricane as dependent on its movement*", arXiv preprint arXiv* :1604.05119.

Mathew, S., Natesan, U., Latha, G., Venkatesan, R., Rao, R.R. and Ravichandran, M. (2018), "Observed warming of sea surface temperature in response to tropical cyclone Thane in the Bay of Bengal", *Current Sci.*, **114**(7), 1407.

Maneesha, K., Murty, V.S.N., Ravichandran, M., Lee, T., Yu, W. and McPhaden, M.J. (2012), "Upper ocean variability in the Bay of Bengal during the tropical cyclones Nargis and Laila", *Progress in Oceanography*, **106**, 49-61.

Maneesha, K., Sadhuram, Y. and Prasad, K.V.S.R. (2015), "Role of upper ocean parameters in the genesis, intensification and tracks of cyclones over the Bay of Bengal", *J. Operational Oceanography*, **8**(2), 133-146.

McPhaden, M.J., Busalacchi, A.J., Cheney, R., Donguy, J.R., Gage, K.S., Halpern, D., Ji, M., Julian, P., Meyers, G., Mitchum, G.T. and Niiler, P.P. (1998), "The tropical ocean-global atmosphere observing system: A decade of progress", *J. Geophys. Res: Oceans*, **103**(7), 14169-14240.

Nath, S., Kotal, S.D. and Kundu, P.K. (2016), "Decadal variation of ocean heat content and tropical cyclone activity over the Bay of Bengal", *J. Earth Syst. Sci.*, **125**(1), 65-74.

Palmen, E. (1948), "On the formation and structure of tropical hurricanes", *Geophysica*, **3**(1), 26-38.

Reddy, B.N.K., Venkatesan, R., Osuri, K.K., Mathew, S., Kadiyam, J. and Joseph, K.J. (2018), "Comparison of AMSR-2 wind speed and sea surface temperature with moored buoy observations over the Northern Indian Ocean", *J. Earth Syst. Sci.*, **127**(1), 14..

Sadhuram, Y., Maneesha, K. and Murty, T.R. (2010), "Importance of upper ocean heat content in the intensification and translation speed of cyclones over the Bay of Bengal", *Current Sci.*, **99**(9), 1191-1194.

Sadhuram, Y. and Murthy, T.V. (2006), "Estimation of tropical cyclone heat potential in the Bay of Bengal and its role in the genesis and intensification of storms".

Srinivasa Kumar, T., Venkatesan, R., Vedachalam, N., Padmanabham, J. and Sundar, R. (2016), "Assessment of the reliability of the Indian Tsunami early warning system", *Marine Technol. Soc. J.*, **50**(3), 92-108.

Venkatesan, R., Arul Muthiah, M., Ramesh, K., Ramasundaram, S., Sundar, R. and Atmanand, M.A. (2013), "Satellite communication systems for ocean observational platforms: Societal importance and challenges", *J. Ocean Technol.*, **8**(3).

Venkatesan, R., Kadiyam, J., Senthil Kumar, P., Lavanya, R. and Vedaprakash, L. (2017), "Marine biofouling on moored buoys and sensors in the Northern Indian Ocean", *Mar. Technol. Soc. J.*, **51**(2), 22-30.

Venkatesan, R., Mathew, S., Vimala, J., Latha, G., Muthiah, M.A., Ramasundaram, S., Sundar, R., Lavanya, R. and Atmanand, M.A. (2014), "Signatures of very severe cyclonic storm Phailin in met–ocean parameters observed by moored buoy network in the Bay of Bengal", *Current Sci.*, 589-595.

Venkatesan, R., Ramasundaram, S., Sundar, R., Vedachalam, N., Lavanya, R. and Atmanand, M.A. (2015), "Reliability assessment of state-of-the-art real-time data reception and analysis system for the Indian seas", *Mar. Technol. Soc. J.*, 49(3), 127-134.

Venkatesan, R., Senthilkumar, P., Vedachalam, N. and Murugesh, P. (2017), "Biofouling and its effects in

sensor mounted moored observatory system in Northern Indian Ocean", *Int. Biodeterioration & Biodegradation*, **116**, 198-204.

Venkatesan, R., Sundar, R., Vedachalam, N. and Jossia Joseph, K. (2016), "India's Ocean observation network: Relevance to society", *Mar. Technol. Soc. J.*, **50**(3), 34-46.

Venkatesan, R., Shamji, V.R., Latha, G., Mathew, S., Rao, R.R., Muthiah, A. and Atmanand, M.A. (2013), "In situ ocean subsurface time-series measurements from OMNI buoy network in the Bay of Bengal", *Current Sci.*, 1166-1177.

Venkatesan, R., Vedachalam, N., Muthiah, M.A., Sundar, R., Kesavakumar, B., Ramasundaram, S. and Jossia Joseph, K. (2018), "Reliability metrics from two decades of Indian Ocean moored buoy observation network", *Mar. Technol. Soc. J.*, **52**(3), 71-90.

Venkatesan, R., Vedachalam, N., Murugesh, P., Kaliyaperumal, P., Kalaivanan, C.K., Gnanadhas, T. and Atmanand, M.A. (2015), "Reliability analysis and integrity management of instrumented buoy moorings for monitoring the Indian Seas", *Underwater Technol.*, **33**(2), 115-126.

Venkatesan, R., Vedachalam, N., Muthiah, M.A., Kesavakumar, B., Sundar, R. and Atmanand, M.A. (2015), "Evolution of reliable and cost-effective power systems for buoys used in monitoring Indian seas", *Mar. Technol. Soc. J.*, **49**(1), 71-87

Venkatesan, R., Vengatesan, G., Vedachalam, N., Muthiah, M.A., Lavanya, R. and Atmanand, M.A. (2016), "Reliability assessment and integrity management of data buoy instruments used for monitoring the Indian Seas", *Appl. Ocean Res.*, **54**, 1-11.

Vedachalam, N., Ravindran, M. and Atmanand, M.A. (2019), "Technology developments for the strategic Indian blue economy", *Marine Georesources & Geotechnology*, **37**(7), 828-844.

Vissa, N.K., Satyanarayana, A.N.V. and Kumar, B.P. (2012), "Response of upper ocean during passage of MALA cyclone utilizing ARGO data", *Int. J. Appl. Earth Observ. Geoinformation*, **14**(1), 149-159.

Weller, R.A., Farrar, J.T., Buckley, J., Mathew, S., Venkatesan, R., Lekha, J.S., Chaudhuri, D., Kumar, N.S. and Kumar, B.P. (2016), "Air-sea interaction in the Bay of Bengal", *Oceanography*, **29**(2), 28-37.

AK